Molecular mechanisms involved in renal injury-repair and ADPKD progression

Formica, C.

CHAPTER 2

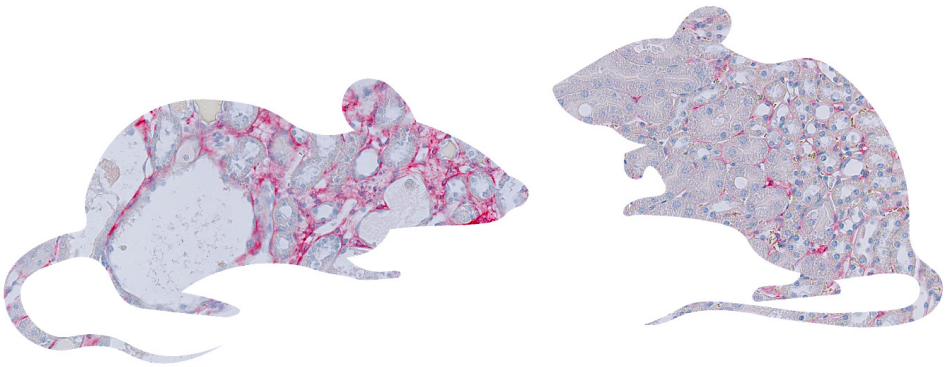

Four-Jointed knock-out delays renal failure in an ADPKD model with kidney injury

Chiara Formica[1], Hester Happé[1], Kimberley A.M. Veraar[2], Andrea Vortkamp[3], Marion Scharpfenecker[2], Helen McNeill[4], Dorien J.M. Peters[1]

[1]Department of Human Genetics, Leiden University Medical Center, The Netherlands

[2]Department of Pathology, Leiden University Medical Center, The Netherlands

[3]Department of Developmental Biology, Centre of Medical Biotechnology, Essen, Germany

[4]Department of Developmental Biology, Washington University School of Medicine, St. Louis, USA; Department of Molecular Genetics, University of Toronto, Canada; Lunenfeld-Tanenbaum Research Institute, Sinai Health System, Toronto, Canada

J Pathol. 2019 Sep;249(1):114-125

Abstract

Autosomal Dominant Polycystic Kidney Disease (ADPKD) is characterized by the development of fluid-filled cysts in the kidneys which lead to end-stage renal disease (ESRD). In the majority of cases, the disease is caused by a mutation in the *Pkd1* gene. In a previous study, we demonstrated that renal injury can accelerate cyst formation in *Pkd1* knock-out (KO) mice. In that study, we found that Four-jointed (FJX1), an upstream regulator of planar cell polarity and the Hippo pathway, was aberrantly expressed in *Pkd1* KO mice compared to wild-type after injury. Therefore we hypothesized a role for FJX1 in injury/repair and cyst formation. We generated single and double deletion mice for *Pkd1* and *Fjx1*, and we induced toxic renal injury using the nephrotoxic compound 1,2-dichlorovinyl-cysteine (DCVC). We confirmed that nephrotoxic injury can accelerate cyst formation in *Pkd1* mutant mice. This caused *Pkd1* KO mice to reach ESRD significantly faster; unexpectedly, double KO mice survived significantly longer. Indeed, cyst formation was comparable in both models, but we found significantly lower fibrosis and macrophage infiltrates in double KO mice. Taken together, these data suggest that *Fjx1* disruption protects the cystic kidneys against kidney failure by reducing inflammation and fibrosis. Moreover, we describe, for the first time, an interesting (yet unidentified) mechanism that partially discriminates cyst growth from fibrogenesis.

Introduction

Autosomal Dominant Polycystic Disease (ADPKD) is a genetic disease caused in the majority of the cases by a mutation in the *Pkd1* gene, which encodes Polycystin 1, and in the remaining cases by a mutation in the *Pkd2* gene, encoding Polycystin 2[1]. The hallmark of this disease is the formation of fluid-filled cysts in the kidneys, which slowly grow and progressively disrupt the renal parenchyma, ultimately leading to kidney failure[1,2]. The exact mechanisms behind cyst formation are still elusive, and effective therapies are still missing, although the Vasopressin V2R antagonist Tolvaptan has become recently available for selected patients[3-5].

Recently, our group showed that a substantial proportion of genes typically deregulated in ADPKD also plays a role in injury-repair mechanisms[6]. Indeed, less than a decade ago, injury has emerged as an important player in cyst formation and progression, and now it is considered a "modifier" of ADPKD[7]. Several other groups and we described that both nephrotoxic[8] and ischemic injury, as well as unilateral nephrectomy[9-12], were able to speed up cyst formation and progression, reinforcing the link between ADPKD progression and injury. In particular, we identified one gene, *Four-jointed box1* (*Fjx1*), as an interesting player in these processes. In our study, *Fjx1* showed aberrant expression during both the injury-repair phase and cyst progression in *Pkd1* KO mice compared with wild-type mice[8]. Moreover, *Fjx1* is implicated with two important pathways normally aberrant in ADPKD: planar cell polarity (PCP) and the Hippo pathway.

FJX1 is the mammalian homolog of the *Drosophila* protein Fj, discovered for its pivotal role in the correct development of leg joints, wings and eyes[9,10]. Fj regulates the interaction of Fat (Ft) with Dachsous (Ds), which controls PCP signalling, most likely in parallel with the Frizzled signals[10-12]. *Fj* mutant *Drosophila* models have a clear alteration of PCP, while *Fjx1* KO mice do not show any evident morphological defects in the kidneys or other organs[13,14]. However, deleting the target of FJX1, *Fat4*, leads to loss of PCP in the inner ear, cochlea and the neural tube, and mild cyst formation in mouse kidney. Loss of both, *Fat4* and *Fjx1,* slightly aggravates the phenotype suggesting that FJX1 may also act via Fat4-independent pathways. Yet, the effect of *Fjx1* in a *Pkd1* mutant context is to date unknown[14].

In *Drosophila,* Fj is also an upstream regulator of the Hippo pathway, through its downstream target Ft. The Hippo pathway regulates proliferation and tissue size through the activity of the final effector and transcriptional co-activator Yorki (Yki)[15-16]. In mammals, there are two *Yki* orthologs: *Yes-associated protein 1* (*Yap1*) and *transcriptional coactivator with PDZ-binding motif* (*Wwtr1* or *Taz*). When the Hippo pathway is active, YAP1 and TAZ are phosphorylated and retained in the cytoplasm, preventing their nuclear translocation and transcriptional activity. In ADPKD, YAP and TAZ activity is upregulated in the cyst-lining

epithelium as indicated by their nuclear localization, suggesting a role for this pathway in cyst progression[17]. In mammals, regulation of the Hippo pathway by FAT4 has recently been shown in the prenatal heart[18]; however, whether this regulatory mechanism also takes place in the kidneys is not clear[14,19].

This study aims to investigate the role of FJX1 during ADPKD progression, particularly after kidney injury and the involvement of the PCP and Hippo pathways. We show that mice that are double mutant for *Fjx1* and *Pkd1* display cyst formation comparable to that of single *Pkd1* KO mice but survive longer. This effect was probably not due to differences in PCP and the Hippo pathway, which were not affected by *Fjx1* deletion, but rather due to reduced fibrosis and macrophage infiltration in the double KO mice. We also show a reduction of fibrosis which is independent of cyst formation. Indeed, in our study, reduced fibrogenesis is directly caused by *Fjx1* deletion and not an indirect consequence of the improved cystic phenotype.

Materials and Methods

Animal Models

All the animal experiments were evaluated and approved by the local animal experimental committee of the Leiden University Medical Centre and the Commission Biotechnology in Animals of the Dutch Ministry of Agriculture. The kidney specific tamoxifen-inducible *Pkd1*-deletion mouse model (*Pkd1*-cKO) and the *Fjx1*$^{-/-}$ (*Fjx1* KO) has been described previously[13,20]. By cross-breeding *Pkd1*-cKO with the *Fjx1* KO mice, we generated the *Fjx1*$^{-/-}$/*Pkd1*-cKO double KO mouse model (double KO). Inactivation of the *Pkd1* gene was achieved by oral administration of tamoxifen in adult mice (13 to 14 weeks old). Renal injury was induced a week after gene disruption by a single intraperitoneal injection of S-(1,2-dichlorovinyl)-L-cysteine (DCVC) or vehicle. Injury was evaluated by measurement of blood urea nitrogen (BUN) level after 40 hours, as described before[8]. More detailed protocols in Supplementary materials.

Immunohistochemistry

Formalin-fixed paraffin-embedded kidneys were sectioned at 4 µm thickness. Sections were stained with Periodic acid-Schiff (PAS) to determine the cystic index (CI) and with Picro Sirius Red (PSR) to determine fibrotic index. Kidney slides were also stained for αSMA, F4/80, YAP, pSTAT3, GM130. More detailed protocols in Supplementary materials.

qPCR

Snap-frozen kidneys were homogenized using Magnalyser technology (Roche). Total RNA was isolated using Tri-Reagent (Sigma-Aldrich). cDNA synthesis was performed using the Transcriptor First Strand cDNA Synthesis Kit (Roche), and qPCR was done using 2× FastStart SYBR-Green Master (Roche) according to the manufacturer's protocol. Primer sequences are provided in Supplementary Table 1. Gene expression was normalized to *Hprt* and fold-change was used for representation in the graphs.

Statistical Analysis

Data were analysed using ANOVA in GraphPad Prism 8.00 for Windows and linear-mixed effects models in IBM SPSS Statistics for Windows, version 23.

Results

Mice double KO for *Pkd1* and *Fjx1* survive longer after toxic tubular damage compared with mice single KO for *Pkd1*.

Inactivation of the *Pkd1* gene was achieved by oral administration of tamoxifen in adult mice. This type of mouse model is characterized by a relatively slow cyst growth that allows having reasonable time windows for the study of the different steps of disease progression. We showed previously that upon nephrotoxic injury cyst initiation is faster in mice with *Pkd1* deletion compared with the non-injured group[8]. Using the same injury model, we administered the nephrotoxic compound DCVC to Wt, *Pkd1* KO, *Fjx1* KO and double KO mice (Figure 1A). We used PBS injection as a control (vehicle group). At 40 h upon DCVC injections, renal injury was confirmed by a substantial rise in the BUN level in all mice, which returned to baseline after 1 week, suggesting a full recovery of the kidney function with no differences among the genotypes (Figure 1B).

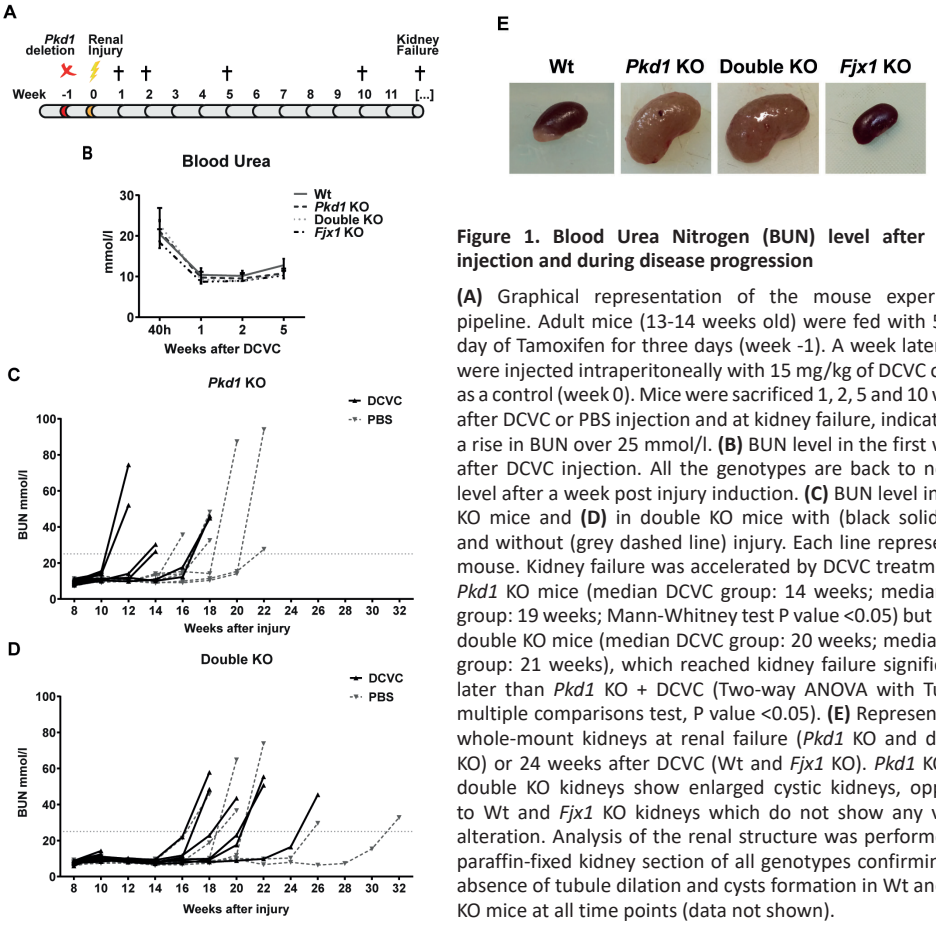

Figure 1. Blood Urea Nitrogen (BUN) level after DCVC injection and during disease progression

(A) Graphical representation of the mouse experiment pipeline. Adult mice (13-14 weeks old) were fed with 5 mg/day of Tamoxifen for three days (week -1). A week later they were injected intraperitoneally with 15 mg/kg of DCVC or PBS as a control (week 0). Mice were sacrificed 1, 2, 5 and 10 weeks after DCVC or PBS injection and at kidney failure, indicated by a rise in BUN over 25 mmol/l. **(B)** BUN level in the first weeks after DCVC injection. All the genotypes are back to normal level after a week post injury induction. **(C)** BUN level in *Pkd1* KO mice and **(D)** in double KO mice with (black solid line) and without (grey dashed line) injury. Each line represents a mouse. Kidney failure was accelerated by DCVC treatment in *Pkd1* KO mice (median DCVC group: 14 weeks; median PBS group: 19 weeks; Mann-Whitney test P value <0.05) but not in double KO mice (median DCVC group: 20 weeks; median PBS group: 21 weeks), which reached kidney failure significantly later than *Pkd1* KO + DCVC (Two-way ANOVA with Tukey's multiple comparisons test, P value <0.05). **(E)** Representative whole-mount kidneys at renal failure (*Pkd1* KO and double KO) or 24 weeks after DCVC (Wt and *Fjx1* KO). *Pkd1* KO and double KO kidneys show enlarged cystic kidneys, opposite to Wt and *Fjx1* KO kidneys which do not show any visible alteration. Analysis of the renal structure was performed on paraffin-fixed kidney section of all genotypes confirming the absence of tubule dilation and cysts formation in Wt and *Fjx1* KO mice at all time points (data not shown).

Pkd1 KO mice injected with DCVC reached end-stage renal disease (ESRD) around 14 weeks after injury. This was significantly earlier than in the vehicle group, which survived for about 19 weeks, in accordance with previously generated data (Figure 1C)[8]. Surprisingly, we observed that the double KO mice did not show a difference between DCVC and vehicle treatment with a median survival of 20 and 21 weeks, respectively (Figure 1D). When compared with *Pkd1* KO mice, double KO mice survived significantly longer after injury, indicating that the lack of *Fjx1* improved survival of double KO mice upon renal damage.
Both Wt and *Fjx1* KO mice subjected to renal injury did not develop cysts still 24 weeks after DCVC, the time point when mice were sacrificed (Figure 1E and data not shown).

Knocking-out *Fjx1* in *Pkd1* mutant mice does not affect cyst formation

Since renal injury accelerates cyst formation in *Pkd1* KO mice[8,21-24], we wondered whether prolonged survival observed in the double KO group treated with DCVC could be due to delayed cyst initiation. We measured the cystic index in kidneys from *Pkd1* KO and double KO mice at 10 weeks after DCVC injection when mice start to show a mild cystic phenotype. We compared *Pkd1* KO and double KO mice with and without DCVC, and did not find any difference in the cystic index, and two kidneys weight to body weight (2KW/BW) ratio's between the genotypes at this time point (Figure 2A-C). Thus, the initiation of cyst formation is not different in the two models, suggesting a role in cyst growth.

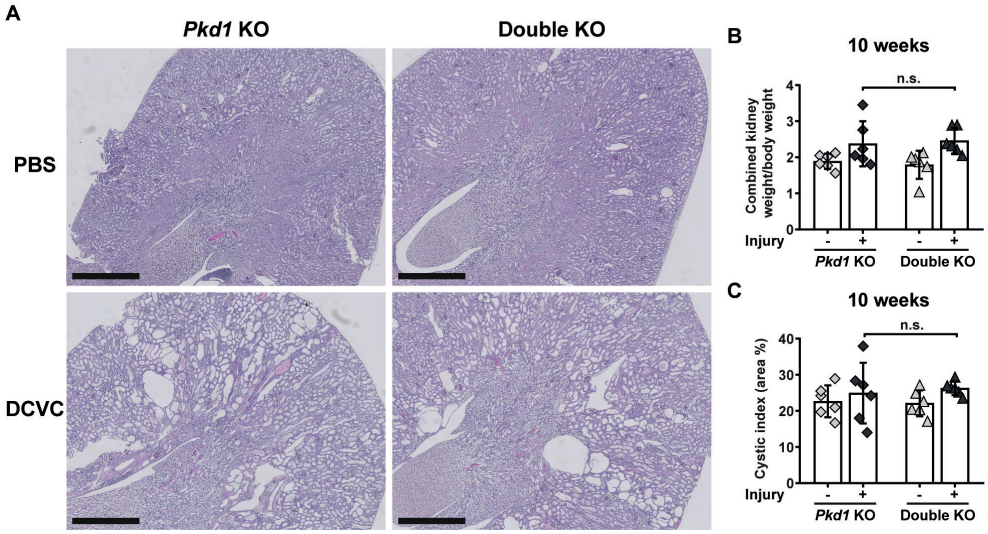

Figure 2. Cysts formation at 10 weeks after DCVC

(A) Representative Periodic Acid Schiff (PAS) staining of *Pkd1* KO and double KO mice at 10 weeks after DCVC, showing comparable cyst formation in the two genotypes. Scale bars, 1 mm. **(B)** Evaluation of kidney size at 10 weeks time-point in *Pkd1* KO and double KO mice with and without injury using two kidney weight/body weight ratio. **(C)** Cystic index at 10 weeks time-point in *Pkd1* KO and double KO mice with and without injury. Each symbol shows data from one mouse. Mean ± SD. Two-way ANOVA with Tukey's multiple comparisons test.

This is also evident when ESRD kidneys are compared. Indeed, *Pkd1* KO mice injected with DCVC, which reach ESRD faster, had a shorter phase of cyst growth and displayed mainly small cysts at kidney failure. Conversely, double KO mice, which have a slower progression to ESRD and therefore a longer phase of cyst growth, show frequently larger cysts (Figure 3A, B). Thus, our data suggest that FJX1 is not directly involved in cyst formation and that prolonged survival of the double KO mice cannot be explained by delayed cyst formation.

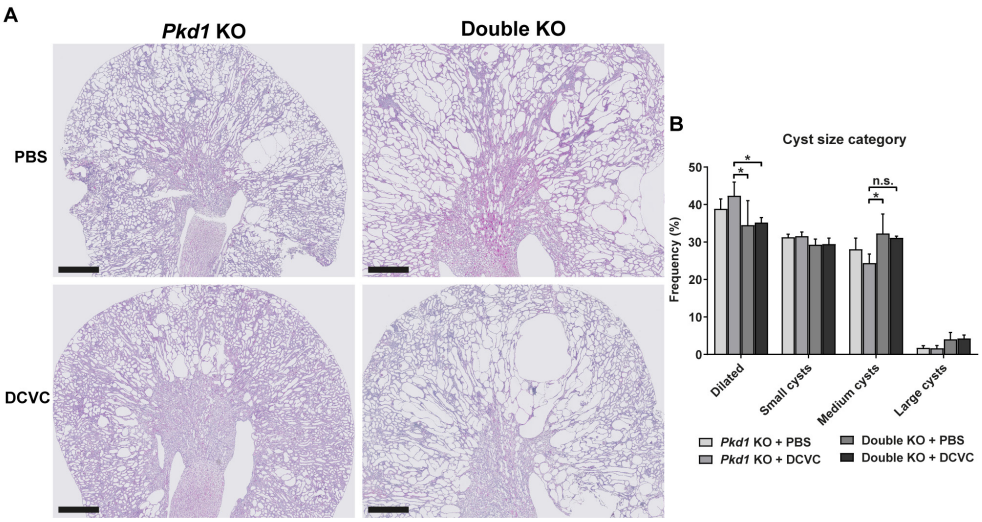

Figure 3. Cysts size at kidney failure

(A) Representative PAS staining of *Pkd1* KO and double KO mice at kidney failure. Scale bars, 1 mm. **(B)** Quantification of cysts size frequency in *Pkd1* KO and double KO mice with and without injury. Data represent the mean of 4 mice ± SD. Three-way ANOVA (P value <0.0001) with Tukey's multiple comparisons test. * P value <0.05.

Chronic injury caused by cyst formation leads to differences in injury markers expression, fibrosis and inflammatory responses in double KO compared with *Pkd1* KO mice

Cyst formation is accompanied by inflammation and fibrosis which ultimately leads to complete loss of renal function. As changes in these processes might affect survival, we analysed whether *Fjx1* deletion altered the expression of injury markers, fibrosis and inflammation.

The expression of the well-established kidney injury molecule *Kim1* (*Havcr1*)[25] was analysed using qPCR. We observed increased *Kim1* expression already at 10 weeks after DCVC injection in *Pkd1* KO and in double KO mice, a time-point when dilation of tubules and small cysts were evident. In contrast, Wt and *Fjx1* KO mice, which do not develop a renal phenotype after DCVC injection, did not show increased *Kim1* expression, reinforcing the idea of cyst-induced chronic injury (Figure 4A). Interestingly, at kidney failure, *Kim1* expression was significantly higher in *Pkd1* KO mice compared to double KO (Figure 4B).

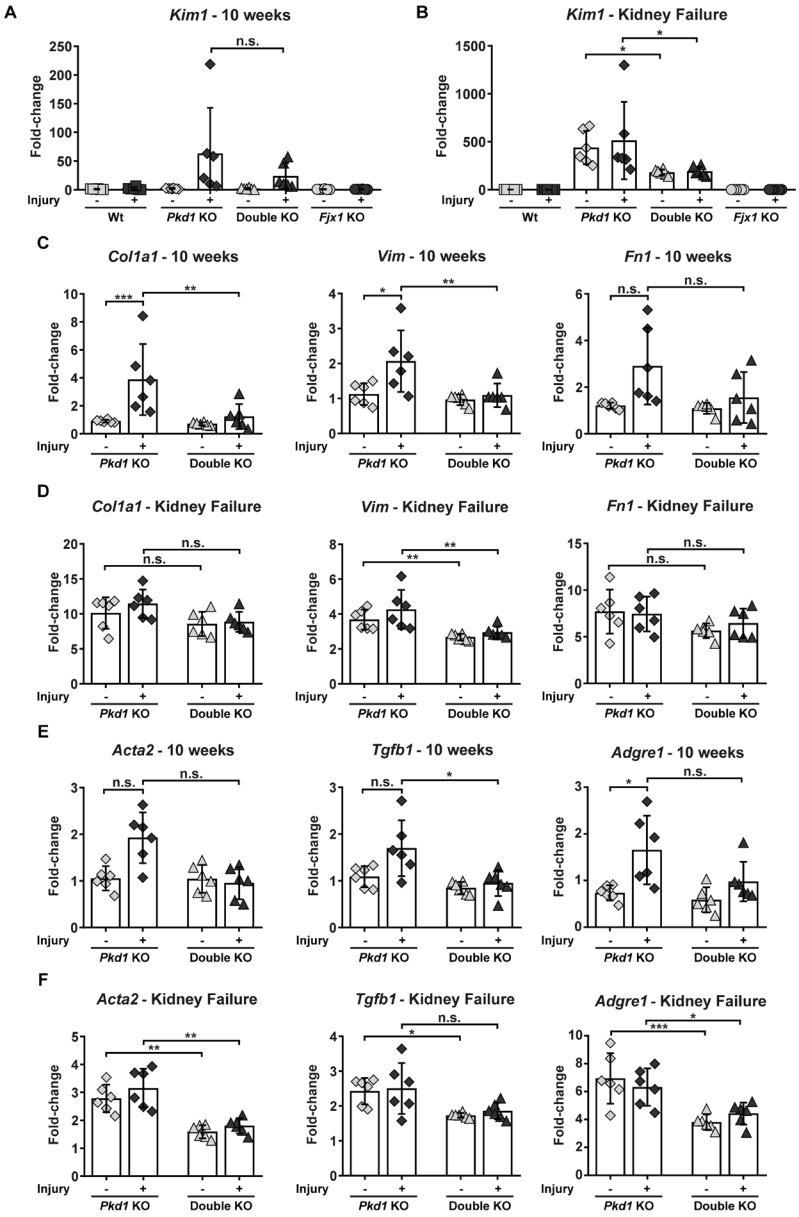

Figure 4. Expression of genes involved in injury-repair in *Pkd1* KO and double KO mice

(A) Gene expression of *Kim1* (*Havcr1*) at 10 weeks after DCVC injection. Both *Pkd1* KO and double KO have a significant increase of *Kim1* expression compared to the PBS groups and the Wt and *Fjx1* KO with and without injury (significance not shown on graph), but not compared to each other. **(B)** Gene expression of *Kim1* at kidney failure after DCVC injection (significance to Wt and *Fjx1* KO not shown on graph). **(C)** Gene expression of *Col1a1*, *Vim* and *Fn1* at 10 weeks after DCVC injection. **(D)** Gene expression of *Col1a1*, *Vim* and *Fn1* at kidney failure. **(E)** Gene expression of *Acta2*, *Tgfb1* and *Adgre1* (F4/80) at 10 weeks after DCVC injection. **(F)** Gene expression of *Acta2*, *Tgfb1* and *Adgre1* at kidney failure. Each symbol shows data from one mouse. Mean ± SD. Two-way ANOVA with Tukey's multiple comparisons test. * P value <0.05; ** P value <0.01; *** P value <0.001.

When we analysed fibrogenesis at 10 weeks after DCVC and kidney failure, expression of alpha-1 type I collagen (*Col1a1*) and Vimentin (*Vim*) was significantly reduced in the double KO compared to *Pkd1* KO at 10 weeks after DCVC, both at the mRNA (Figure 4C, D) and protein levels (Figure 5A, B); expression of Fibronectin (*Fn1*) showed a similar trend (Figure 4C, D). Interestingly, while in *Pkd1* KO mice the expression of these genes was significantly correlated with kidney size, this was not observed in the double KO mice, suggesting that in these mice cyst progression and fibrosis are two independent events (Supplementary Figure 1). Likewise, the expression of transforming growth factor beta-1 (*Tgfb1*), was significantly less in double KO compared to *Pkd1* KO mice at 10 weeks and at kidney failure. Also, double KO mice at 10 weeks had tendentially lower alpha-smooth muscle actin (*Acta2*) transcript and significantly less αSMA positive area (Figure 4E, F; Figure 5C, D).

To characterize the inflammatory response, we looked at the expression of the macrophage marker *Adgre1* (F4/80) and found it to be significantly less expressed in double KO compared to *Pkd1* KO mice at kidney failure (Figure 4E, F). At 10 weeks after DCVC *Adgre1* showed a trend but at the protein level F4/80 expression was significantly reduced in double KO mice (Figure 5E, F). We also checked the expression of *Jak2* and *Stat1*, involved in the transduction of a series of signals, like growth factors and cytokines in response to injury[26]. We found significantly lower expression in double KO compared to *Pkd1* KO mice (Figure 5G, H). On the other hand, Stat3 activation, known to be involved in cyst growth[27], was not significantly different between the two genotypes, supporting the idea that FJX1 role is related to the inflammatory/fibrotic response and not to cyst formation (Supplementary Figure 2). These results indicate that the lack of *Fjx1* leads to a reduced inflammatory/fibrotic response which translates into a longer survival after DCVC administration.

Investigation of pathways involved in renal fibrosis

We also studied the expression of key genes of several pathways known to be involved in renal fibrosis, such as Notch[28,29], Hedgehog[30,31], Wnt[32,33], hypoxia[34-38] and Egf[39-41]. However, we could not find any differences between the double KO and *Pkd1* KO mice, except for Pdgfb (Supplementary Figure 3) and Wnt target genes. Indeed, *Axin2*, *Cd44*, *Ccnd1* (Figure 6A, B) and to certain extent *Myc* (Supplementary Figure 4), showed significantly lower expression in double KO compared with *Pkd1* KO mice, both at 10 weeks after DCVC and at kidney failure, suggesting a reduced activation of the canonical Wnt signalling in the absence of *Fjx1*.

Mice double KO for *Pkd1* and *Fjx1* show less sensitivity to DCVC induced injury than mice single KO for *Pkd1*

To further investigate the role of FJX1 in injury, we performed a pilot experiment in which mice treated with DCVC were sacrificed after 24 h, 48 h and 72 h, i.e. during the

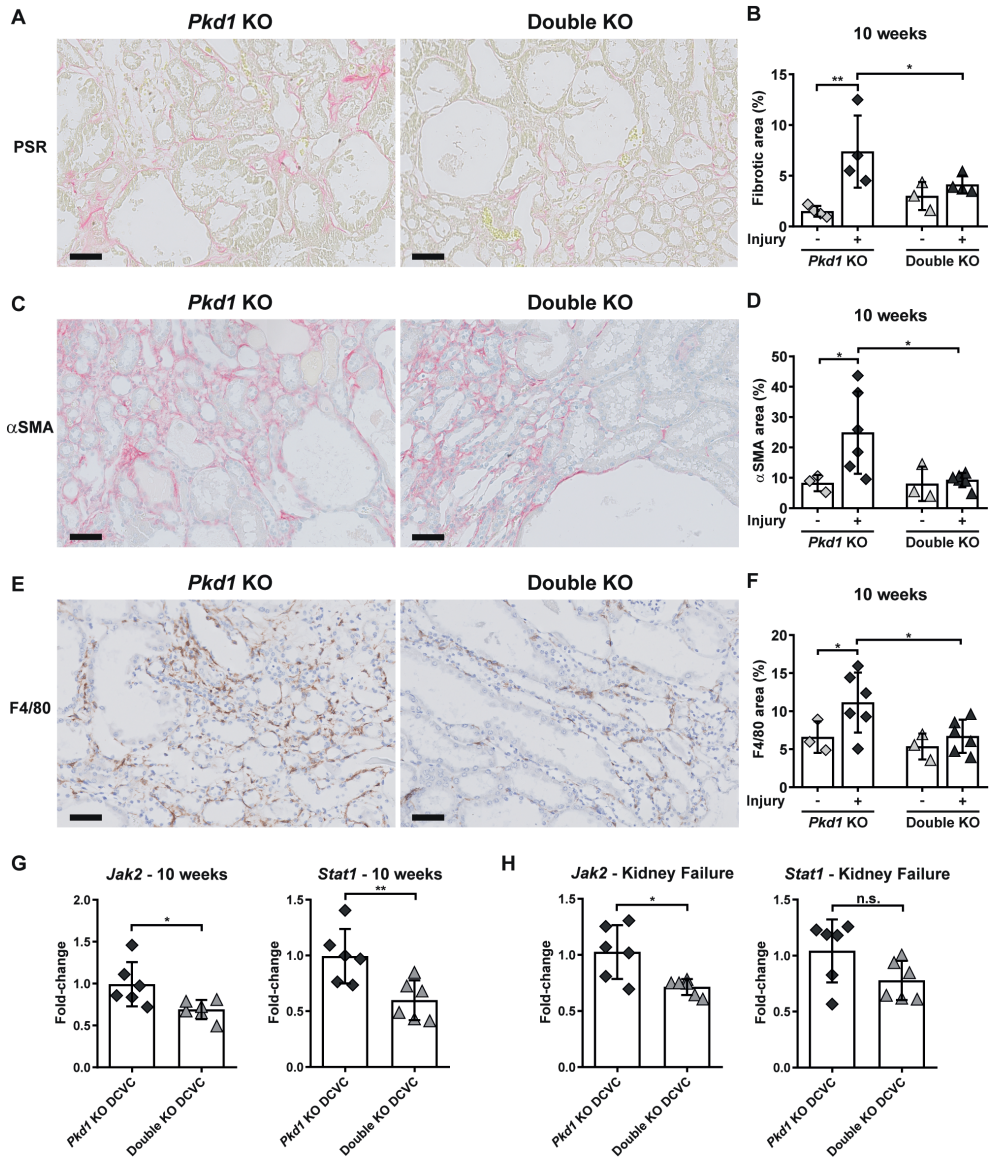

Figure 5. Fibrosis, fibroblast activation and macrophage infiltrates in *Pkd1* KO and double KO mice

(A) Representative Picro Sirius Red (PSR) staining of *Pkd1* KO and double KO mice at 10 weeks after DCVC. Scale bars, 50 µm. **(B)** Quantification of PSR staining in the cortico-medullary region. **(C)** Representative αSMA staining of *Pkd1* KO and double KO mice at 10 weeks after DCVC. Scale bars, 50 µm. **(D)** Quantification of αSMA staining in the cortico-medullary region. **(E)** Representative F4/80 staining of *Pkd1* KO and double KO mice at 10 weeks after DCVC. Scale bars, 50 µm. **(F)** Quantification of F4/80 staining in the cortico-medullary region. Each symbol is a mouse and data represent the mean ± SD. Two-way ANOVA with Tukey's multiple comparisons test. * P value <0.05; ** P value <0.01. **(G)** Gene expression of *Stat1* and *Jak2* at 10 weeks after DCVC in *Pkd1* KO and double KO mice. **(H)** Gene expression of *Stat1* and *Jak2* at kidney failure in *Pkd1* KO and double KO mice treated with DCVC. Each symbol shows data from one mouse. Mean ± SD. Unpaired t-test. * P value <0.05; ** P value <0.01.

nephrotoxin-induced acute injury phase. At all time-points, we found a trend consistent with that observed in the cyst-induced chronic injury, showing that the *Kim1* expression was less in double KO mice than in *Pkd1* KO. At 1 week after DCVC *Kim1* expression is strongly reduced in both genotypes suggesting that the DCVC-induced acute injury is largely repaired in the first week (Supplementary Figure 5). In line with the findings from the chronic injury experiments, the expression of genes involved in fibrogenesis, such as *Cola1a*, *Vim* and *Fn1,* was lower in double KO compared with *Pkd1* KO mice (Supplementary Figure 5).
Together with the results observed during the cyst-induced chronic injury, these data suggest that the lack of *Fjx1* leads to a reduced sensitivity to DCVC-induced injury.

PCP is altered in *Pkd1* mutant mice after injury but is not significantly affected by the lack of *Fjx1*

Tissue injury causes inversion or loss of PCP in epithelial cells, which recovers during the repair phase[42]. *Fj* has been described as an important PCP gene in *Drosophila* as is *Fjx1* in mammals, in particular in the regulation of the brain architecture[13] and inner ear polarity[14]. Therefore we decided to characterize renal PCP at 1 week after injury in *Pkd1* KO and double KO mice.
The levels of expression of *Fat4* and its ligand *Dchs1*[43] were unchanged by *Fjx1* KO (Figure 6C) suggesting that, at the expression level, the Fat/Ds PCP pathway was unaltered in kidneys of mutant mice. We also used the Golgi position to assess the degree of polarity perturbation in tubular cells (Figure 6D). Although Golgi position is not a direct read-out of PCP core proteins, it is found to be aberrant when PCP genes are knocked-out[44], and is also associated with loss of directed secretion, cell polarity and wound healing capacity[45].
We confirmed that altered polarity was associated with loss of *Pkd1* and kidney injury already at the pre-cystic stage, with a significantly higher aberrant Golgi position in *Pkd1* KO and double KO mice compared with Wt and *Fjx1* KO. However, we could not identify any difference between double KO and *Pkd1* KO or between Wt and *Fjx1* KO (Figure 6E), indicating that *Fjx1* did not contribute to an altered PCP.

The effect of *Fjx1* on injury response is not mediated by the Hippo pathway

FJX1 is thought to be an upstream regulator of the Hippo pathway through the activity of FAT4[46]. The Hippo pathway is pivotal in the regulation of organ growth, tissue renewal and regeneration[47] but is also deregulated in ADPKD[17]. Therefore, we investigated this pathway in *Pkd1* KO and double KO mice after DCVC treatment.
The Yap staining of kidney sections confirmed the pattern described before in our lab with increased nuclear localization of Yap in the cystic epithelium[17]. However, we could not detect any significant difference between double KO and *Pkd1* KO. Also, neither mRNA levels of *Yap1* and its paralog *Taz*, nor their transcriptional targets, *Amotl2*, *Cyr61*, *Wtip*, *Ctgf*, *Ajuba* (Supplementary Figure 6), showed any significant difference among genotypes.

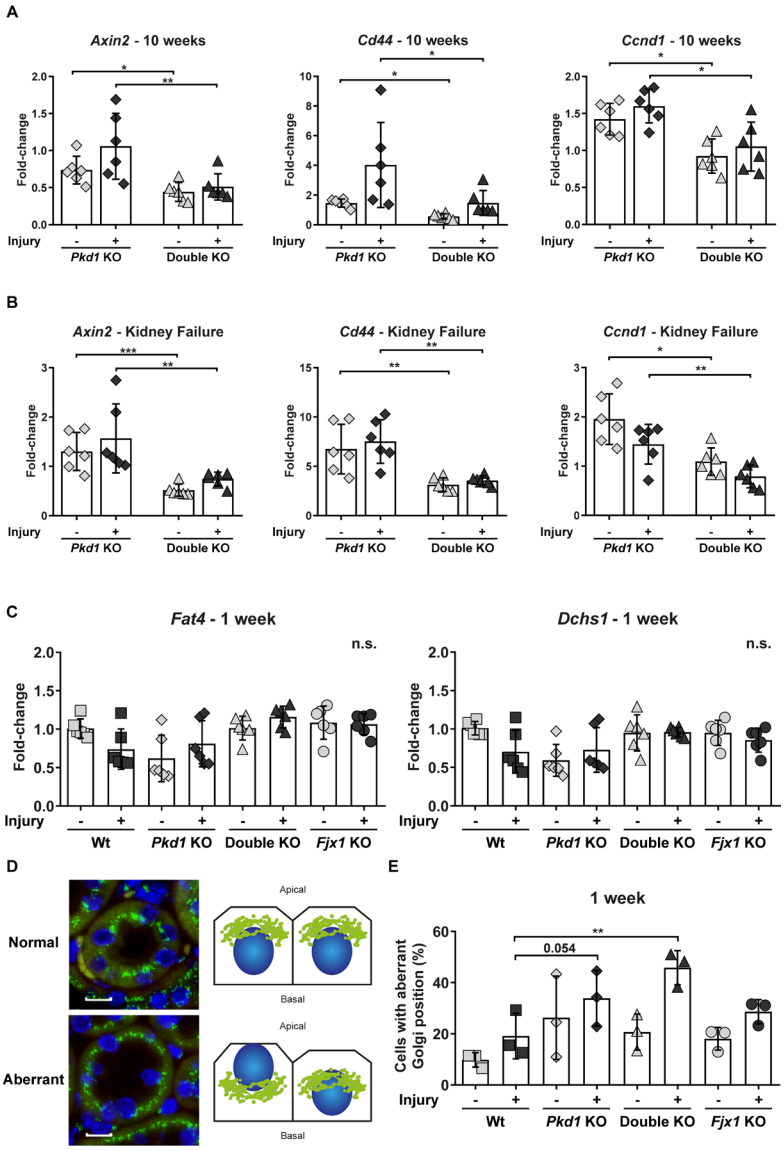

Figure 6. Expression of Wnt pathway target genes and expression level of Fjx1 targets and Golgi position in tubular cells

(A) *Axin2*, *Cd44* and *Ccnd1* mRNA levels at 10 weeks after DCVC injection. **(B)** Gene expression of *Axin2*, *Cd44* and *Ccnd1* at kidney failure. **(C)** Gene expression of *Fat4* and *Dchs1* at 1 week after DCVC injection. Each symbol shows data from one mouse. Mean ± SD. Two-way ANOVA with Tukey's multiple comparisons test. * P value <0.05; ** P value <0.01; *** P value <0.001. **(D)** Representative GM130 (green) staining on kidney tissue. Nuclei are stained in blue. In the normal situation the Golgi is positioned in a peri-centrosomal position at the top of the nucleus towards the lumen of the tubules, but after injury we often observed altered Golgi position. Scale bars, 10 µm. **(E)** Golgi position has been scored from 1 (normal position) to 3 (really abnormal position) in the round shaped tubules in the cortico-medullary region. Results are represented as the percentage of aberrant Golgi position (score ≥2.5) per tubules. Each symbol is the mean ± SD of about 90 tubules scored in a mouse. Two-way ANOVA with Fisher's LSD. ** P value <0.01.

This suggests that despite the clear nuclear localization of Yap in the cystic epithelium this pathway is not responsible for the difference in survival between *Pkd1* KO and double KO mice.

Taken together, these data indicate that knocking-out *Fjx1* does not affect PCP and the Hippo pathway in the kidneys. Therefore, the differences observed in response to injury in double KO mice cannot be explained by the effect of *Fjx1* on one of its canonical targets but suggests the existence of other, yet unknown, FJX1 targets.

Discussion

In this study we showed that nephrotoxic injury can accelerate disease progression in *Pkd1* KO mice but that this effect is abolished in the absence of *Fjx1* expression, allowing the *Pkd1*/*Fjx1* double KO mice to survive on average 5 weeks longer than the single *Pkd1* KO mice. Interestingly, the initiation of cyst formation and cyst growth were not different among the two models, as shown by 2KW/BW ratios and the cystic index. At 10 weeks after DCVC and kidney failure, however, we observed a reduction in injury marker expression together with reduced fibrosis and macrophage infiltration in *Pkd1* KO mice compared with double KO. Therefore, these data suggest that FJX1 does not play a critical role in cyst formation and expansion but seems to be involved in the fibrotic and inflammatory response to injury. As a result, the mice lacking both, *Fjx1* and *Pkd1*, have less fibrosis, which leads to a slower progression to ESRD and longer survival.

Fj is, together with the Ft-Ds cassette, part of a signalling complex, which is involved in the regulation of PCP in *Drosophila*[48-51]. Nevertheless, the absence of *Fjx1* did not alter PCP in the kidneys when compared with Wt mice, or in double KO compared to *Pkd1* KO mice. Although we observed significant deregulation of PCP in pre-cystic kidneys after injury in both single *Pkd1* mutant mice and double KO, the additional deletion of *Fjx1* did not further change the PCP phenotype in the *Pkd1* KO. These results are consistent with the published work of Probst *et al.*[13] showing that *Fjx1* KO mice do not have aberrant PCP in the kidneys but show only defects in neuronal branching. An effect on renal PCP was only seen after knocking-out *Fat4*, a target of FJX1, suggesting a more indirect effect of FJX1 on PCP in mammals[14,19]. We already showed in a previous study that PCP is impaired in *Pkd1* KO mice but not in Wt mice after injury, and that *Pkd1* KO mice injected with DCVC also develop cysts earlier when compared with the PBS group[8]. Whether pre-cystic alterations of PCP are critical for cyst formation is still controversial. Several studies are suggesting that PCP and cilium-associated control of oriented cell division (OCD) as well as convergent extension (CE) are necessary during renal tubular morphogenesis and also during proliferation phases in adult kidneys. Alterations of both OCD and CE are involved in PKD[23,52-54]. However, there are also studies showing that alterations in OCD and CE occur only after cyst formation, or that mutations of PCP-core proteins do not result in cyst formation[55,56]. This means that simple alteration of PCP is not sufficient to start cyst formation but disrupted PCP together with other events, such as injury, presumably increases the likelihood of cyst initiation.

Another pathway altered in ADPKD is the Hippo pathway, which is also regulated via the FJX1 target FAT4. In particular, the pathway's effectors Yap1 and Taz have been associated with cyst formation. We showed in the past that Yap1 accumulates in the nuclei of the cyst-lining epithelium[8,17], and other groups showed how deregulations of YAP1 activity

could induce cyst formation in Zebrafish models[57,58]. Moreover, knocking-out *Taz* in mice leads to glomerular and proximal tubular cyst formation[59-61]. Nevertheless, we did not see an effect of FJX1 on the Hippo pathway when comparing *Pkd1* KO and double KO mice. *Yap1* and *Taz* levels, as well as the levels of several of their target genes, were comparable in the two genotypes throughout disease progression. Also, *Fat4* levels were unchanged by *Fjx1* deletion (data not shown). Currently, clear proof that the FJX1-FAT4-DCHS cassette interaction controls PCP and Hippo pathway in kidneys is still missing[14,19,62].

Once cysts start to form and expand, they compress the surrounding tissue, compromise the normal tubular structure and also interfere with the extracellular compartment. This is accompanied by the expression of injury markers and activation of transcription factors like Stat3, Creb and ERK, known to be involved in ADPKD pathogenesis, and with an increased likelihood of more cyst formation[22,27,63,64]. All these cues are perceived by the organ like a constant injury insult and accompanied by a fibrotic and inflammatory response. Concomitantly, a severe cystic phenotype is associated with renal function decline due to the accumulation of fibrosis and inflammatory infiltrates, which interfere with normal organ function[65,66]. Nonetheless, it is unclear whether inflammation and fibrosis are responsible for or just a consequence of cyst formation. In our study, we observed separation between cyst formation and fibrotic response when *Fjx1* is inactivated. Indeed double KO mice had significantly reduced fibrosis and leukocytes infiltrates compared with *Pkd1* KO mice even though cyst formation was comparable. We could exclude the involvement of some fibrosis-related pathways, such as Notch, Hedgehog, hypoxia and Egfr signalling, while we found a significant reduction of expression of *Pdgfb*, *Tgfb1*, *Jak2* and *Stat1*, and Wnt pathway target genes in double KO compared to *Pkd1* KO mice. Considering the well described role of Tgfb and Wnt pathways in renal fibrosis[32,33,67,68], it is plausible to think that they might be responsible for the reduced fibrosis observed in double KO mice. Indeed, Tgfb can regulate the expression of *Pdgfb*[69], *Fn1* and type I collagen[70,71] all found downregulated in double KO mice. Similarly, Wnt targets *Axin2*[72], *Cd44*[73], *Ccnd1*[74,75] and *Myc*[76] were lower in double KO mice. Further studies are required to link FJX1 with the Tgfb and Wnt pathways mechanistically. An interesting connection between FJX1 and Jak/Stat pathways has been described in the literature, with Fj as the effector of the pleiotropic pathway Jak/Stat in *Drosophila*[10]. Although it is tempting to speculate that this might be the route through which FJX1 modulates the injury response, it is more likely that reduced *Jak2*/*Stat1* levels in the double KO mice mirror a reduced inflammatory response. Overall, these data suggest that FJX1 is involved in the fibrotic/inflammatory response after injury. We also showed that a different response to injury in the double KO mice could also play a role during the acute injury phase between 24 and 72 h after DCVC injection. This is not surprising, considering that *Fjx1* is mainly expressed in the developing kidneys while its expression is almost absent in adult kidneys[77]. Indeed, as for many other developmental genes, injury causes an increase

in expression of *Fjx1*[8]. Yet, the mechanism through which FJX1 is influencing these processes is still unclear.

As the function of FJX1 is still obscure, we cannot exclude that, besides the canonical targets Fat and Dachsous, additional direct targets of FJX1 exist. This is because FJX1 is a Golgi secretory pathway kinase and therefore likely involved in many biological processes, as already shown for its closely related homolog Fam20C[78,79]. Additionally, FJX1 protein undergoes partial proteolytic cleavage at the N-terminus, with the secretion of the resultant fragment that can function as signalling ligand, influencing surrounding cells. FJX1 fusion protein experiments have shown several FJX1 binding sites present in different organs, including kidneys[77]. Therefore, a better understanding of FJX1 functions in mammals might help to explain the effect we unveiled on fibrogenesis.

In conclusion, we show that cyst progression and fibrosis in *Pkd1*/*Fjx1* double KO mice are partially uncoupled and demonstrate a new, yet undefined, role of FJX1 in fibrosis, ultimately resulting in longer survival. Unveiling the underlying molecular mechanism might open the path for future therapies that can specifically target injury-induced fibrosis, and could not only help to slow down ADPKD, but also the progression of other chronic kidney diseases.

Acknowledgements

This work was supported by grants from the People Program (Marie Curie Actions) of the European Union's Seventh Framework Program FP7/2077-2013 under Research Executive Agency Grant Agreement 317246, and by the Dutch Kidney Foundation consortium grant (CP10.12 -DIPAK). The DIPAK Consortium is an inter-university collaboration in The Netherlands that is established to study Autosomal Dominant Polycystic Kidney Disease and to develop rational treatment strategies for this disease. Principal investigators are (in alphabetical order): J.P.H. Drenth (Dept. Gastroenterology and Hepatology, Radboud UMC Nijmegen), J.W. de Fijter (Dept. Nephrology, Leiden UMC), R.T. Gansevoort (Dept. Nephrology, UMC Groningen), D.J.M. Peters (Dept. Human Genetics, Leiden UMC), J. Wetzels (Dept. Nephrology, Radboud UMC Nijmegen) and R. Zietse (Dept. Internal Medicine, Erasmus MC Rotterdam).

Author contributions

C.F. (concept design, data acquisition, data interpretation, writing paper), H. H. (concept design), D.J.M.P. (concept design, data interpretation, writing paper), K.A.M.V. (histopathology), M.S. (data interpretation and manuscript reviewing), A.V. and H.M.N. (mice, data discussion, manuscript reviewing).

References

1 Igarashi, P. Genetics and Pathogenesis of Polycystic Kidney Disease. Journal of the American Society of Nephrology 13, 2384-2398, doi:10.1097/01.asn.0000028643.17901.42 (2002).

2 Takiar, V. & Caplan, M. J. Polycystic kidney disease: pathogenesis and potential therapies. Biochim Biophys Acta 1812, 1337-1343, doi:10.1016/j.bbadis.2010.11.014 (2011).

3 Torres, V. E. et al. Tolvaptan in patients with autosomal dominant polycystic kidney disease. N Engl J Med 367, 2407-2418, doi:10.1056/NEJMoa1205511 (2012).

4 Ong, A. C. M. Polycystic kidney disease: Tolvaptan slows disease progression in late-stage ADPKD. Nat Rev Nephrol, doi:10.1038/nrneph.2017.180 (2018).

5 Gansevoort, R. T. et al. Recommendations for the use of tolvaptan in autosomal dominant polycystic kidney disease: a position statement on behalf of the ERA-EDTA Working Groups on Inherited Kidney Disorders and European Renal Best Practice. Nephrol Dial Transpl 31, 337-348, doi:10.1093/ndt/gfv456 (2016).

6 Malas, T. B. et al. Meta-analysis of polycystic kidney disease expression profiles defines strong involvement of injury repair processes. American Journal of Physiology - Renal Physiology 312, F806-F817 (2017).

7 Leonhard, W. N., Happe, H. & Peters, D. J. Variable Cyst Development in Autosomal Dominant Polycystic Kidney Disease: The Biologic Context. J Am Soc Nephrol 27, 3530-3538, doi:10.1681/ASN.2016040425 (2016).

8 Happé, H. et al. Toxic tubular injury in kidneys from Pkd1-deletion mice accelerates cystogenesis accompanied by dysregulated planar cell polarity and canonical Wnt signaling pathways. Human Molecular Genetics 18, 2532-2542, doi:10.1093/hmg/ddp190 (2009).

9 Tokunaga, C. & Gerhart, J. C. The effect of growth and joint formation on bristle pattern in D. melanogaster. J Exp Zool 198, 79-95, doi:10.1002/jez.1401980110 (1976).

10 Zeidler, M. P., Perrimon, N. & Strutt, D. I. The four-jointed gene is required in the Drosophila eye for ommatidial polarity specification. Curr Biol 9, 1363-1372, doi:Doi 10.1016/S0960-9822(00)80081-0 (1999).

11 Rawls, A. S., Guinto, J. B. & Wolff, T. The cadherins fat and dachsous regulate dorsal/ventral signaling in the Drosophila eye. Curr Biol 12, 1021-1026 (2002).

12 Casal, J., Lawrence, P. A. & Struhl, G. Two separate molecular systems, Dachsous/Fat and Starry night/Frizzled, act independently to confer planar cell polarity. Development 133, 4561-4572, doi:10.1242/dev.02641 (2006).

13 Probst, B., Rock, R., Gessler, M., Vortkamp, A. & Puschel, A. W. The rodent Four-jointed ortholog Fjx1 regulates dendrite extension. Dev Biol 312, 461-470, doi:10.1016/j.ydbio.2007.09.054 (2007).

14 Saburi, S. et al. Loss of Fat4 disrupts PCP signaling and oriented cell division and leads to cystic kidney disease. Nat Genet 40, 1010-1015, doi:10.1038/ng.179 (2008).

15 Staley, B. K. & Irvine, K. D. Hippo signaling in Drosophila: recent advances and insights. Dev Dyn 241, 3-15, doi:10.1002/dvdy.22723 (2012).

16 Reddy, B. V. V. G. & Irvine, K. D. The Fat and Warts signaling pathways: new insights into their regulation, mechanism and conservation. Development 135, 2827-2838, doi:10.1242/dev.020974 (2008).

17 Happe, H. et al. Altered Hippo signalling in polycystic kidney disease. J Pathol 224, 133-142, doi:10.1002/path.2856 (2011).

18 Ragni, C. V. et al. Amotl1 mediates sequestration of the Hippo effector Yap1 downstream of Fat4 to restrict heart growth. Nat Commun 8, 14582, doi:10.1038/ncomms14582 (2017).

19 Mao, Y. et al. Characterization of a Dchs1 mutant mouse reveals requirements for Dchs1-Fat4 signaling during mammalian development. Development 138, 947-957, doi:10.1242/dev.057166 (2011).

20 Lantinga-van Leeuwen, I. S. et al. Kidney-specific inactivation of the Pkd1 gene induces rapid cyst formation in developing kidneys and a slow onset of disease in adult mice. Hum Mol Genet 16, 3188-3196, doi:10.1093/hmg/ddm299 (2007).

21 Takakura, A. et al. Renal injury is a third hit promoting rapid development of adult polycystic kidney disease. Hum Mol Genet 18, 2523-2531, doi:10.1093/hmg/ddp147 (2009).

22 Leonhard, W. N. et al. Scattered Deletion of PKD1 in Kidneys Causes a Cystic Snowball Effect and Recapitulates Polycystic Kidney Disease. J Am Soc Nephrol 26, 1322-1333, doi:10.1681/ASN.2013080864 (2015).

23 Patel, V. et al. Acute kidney injury and aberrant planar cell polarity induce cyst formation in mice lacking renal cilia. Hum Mol Genet 17, 1578-1590, doi:10.1093/hmg/ddn045 (2008).

24 Bell, P. D. et al. Loss of primary cilia upregulates renal hypertrophic signaling and promotes cystogenesis. J Am Soc Nephrol 22, 839-848, doi:10.1681/ASN.2010050526 (2011).

25 Han, W. K., Bailly, V., Abichandani, R., Thadhani, R. & Bonventre, J. V. Kidney Injury Molecule-1 (KIM-1): a novel biomarker for human renal proximal tubule injury. Kidney Int 62, 237-244, doi:10.1046/j.1523-1755.2002.00433.x (2002).

26 Yang, N. S. et al. Blockage of JAK/STAT signalling attenuates renal ischaemia-reperfusion injury in rat. Nephrol Dial Transpl 23, 91-100, doi:10.1093/ndt/gfm509 (2008).

27 Weimbs, T. & Talbot, J. J. STAT3 Signaling in Polycystic Kidney Disease. Drug Discov Today Dis Mech 10, e113-e118, doi:10.1016/j.ddmec.2013.03.001 (2013).

28 Dees, C. et al. Inhibition of Notch signaling prevents experimental fibrosis and induces regression of established fibrosis. Arthritis Rheum 63, 1396-1404, doi:10.1002/art.30254 (2011).

29 Hu, B. & Phan, S. H. Notch in fibrosis and as a target of anti-fibrotic therapy. Pharmacol Res 108, 57-64, doi:10.1016/j.phrs.2016.04.010 (2016).

30 Hu, L., Lin, X., Lu, H., Chen, B. & Bai, Y. An overview of hedgehog signaling in fibrosis. Mol Pharmacol 87, 174-182, doi:10.1124/mol.114.095141 (2015).

31 Kramann, R. Hedgehog Gli signalling in kidney fibrosis. Nephrol Dial Transplant 31, 1989-1995, doi:10.1093/ndt/gfw102 (2016).

32 Piersma, B., Bank, R. A. & Boersema, M. Signaling in Fibrosis: TGF-beta, WNT, and YAP/TAZ Converge. Front Med (Lausanne) 2, 59, doi:10.3389/fmed.2015.00059 (2015).

33 Tan, R. J., Zhou, D., Zhou, L. & Liu, Y. Wnt/beta-catenin signaling and kidney fibrosis. Kidney Int Suppl (2011) 4, 84-90, doi:10.1038/kisup.2014.16 (2014).

34 Parrish, A. R. The cytoskeleton as a novel target for treatment of renal fibrosis. Pharmacol Therapeut 166, 1-8, doi:10.1016/j.pharmthera.2016.06.006 (2016).

35 Kawakami, T., Mimura, I., Shoji, K., Tanaka, T. & Nangaku, M. Hypoxia and fibrosis in chronic kidney disease: crossing at pericytes. Kidney Int Suppl 4, 107-112, doi:10.1038/kisup.2014.20 (2014).

36 Edeling, M., Ragi, G., Huang, S., Pavenstadt, H. & Susztak, K. Developmental signalling pathways in renal fibrosis: the roles of Notch, Wnt and Hedgehog. Nat Rev Nephrol 12, 426-439, doi:10.1038/nrneph.2016.54 (2016).

37 Ruthenborg, R. J., Ban, J. J., Wazir, A., Takeda, N. & Kim, J. W. Regulation of wound healing and fibrosis by hypoxia and hypoxia-inducible factor-1. Mol Cells 37, 637-643, doi:10.14348/molcells.2014.0150 (2014).

38 Darby, I. A. & Hewitson, T. D. Hypoxia in tissue repair and fibrosis. Cell Tissue Res 365, 553-562, doi:10.1007/s00441-016-2461-3 (2016).

39 Zhuang, S. G. & Liu, N. EGFR signaling in renal fibrosis. Kidney Int Suppl 4, 70-74, doi:10.1038/kisup.2014.13 (2014).

40 Chen, J. et al. EGFR signaling promotes TGFbeta-dependent renal fibrosis. J Am Soc Nephrol 23, 215-224, doi:10.1681/ASN.2011070645 (2012).

41 Terzi, F. et al. Targeted expression of a dominant-negative EGF-R in the kidney reduces tubulo-interstitial lesions after renal injury. J Clin Invest 106, 225-234, doi:10.1172/JCI8315 (2000).

42 Siegel, N. J., Devarajan, P. & Van Why, S. Renal cell injury: metabolic and structural alterations. Pediatr Res 36, 129-136, doi:10.1203/00006450-199408000-00001 (1994).

43 Mao, Y. P., Francis-West, P. & Irvine, K. D. Fat4/Dchs1 signaling between stromal and cap mesenchyme cells influences nephrogenesis and ureteric bud branching. Development 142, 2574-U2569, doi:10.1242/dev.122630 (2015).

44 Caddy, J. et al. Epidermal wound repair is regulated by the planar cell polarity signaling pathway. Developmental cell 19, 138-147, doi:10.1016/j.devcel.2010.06.008 (2010).

45 Yadav, S., Puri, S. & Linstedt, A. D. A primary role for Golgi positioning in directed secretion, cell polarity, and wound healing. Mol Biol Cell 20, 1728-1736, doi:10.1091/mbc.E08-10-1077 (2009).

46 Das, A. et al. Stromal–epithelial crosstalk regulates kidney progenitor cell differentiation. Nature Cell Biology 15, 1035, doi:10.1038/ncb2828 (2013).

47 Piccolo, S., Dupont, S. & Cordenonsi, M. The biology of YAP/TAZ: hippo signaling and beyond. Physiol Rev 94, 1287-1312, doi:10.1152/physrev.00005.2014 (2014).

48 Casal, J., Struhl, G. & Lawrence, P. A. Developmental compartments and planar polarity in Drosophila. Curr Biol 12, 1189-1198 (2002).

49 Yang, C. H., Axelrod, J. D. & Simon, M. A. Regulation of Frizzled by fat-like cadherins during planar polarity signaling in the Drosophila compound eye. Cell 108, 675-688 (2002).

50 Matakatsu, H. & Blair, S. S. Interactions between Fat and Dachsous and the regulation of planar cell polarity in the Drosophila wing. Development 131, 3785-3794, doi:10.1242/dev.01254 (2004).

51 Cho, E. & Irvine, K. D. Action of fat, four-jointed, dachsous and dachs in distal-to-proximal wing signaling. Development 131, 4489-4500, doi:10.1242/dev.01315 (2004).

52 Fischer, E. et al. Defective planar cell polarity in polycystic kidney disease. Nat Genet 38, 21-23, doi:10.1038/ng1701 (2006).

53 Luyten, A. et al. Aberrant regulation of planar cell polarity in polycystic kidney disease. J Am Soc Nephrol 21, 1521-1532, doi:10.1681/ASN.2010010127 (2010).

54 Castelli, M. et al. Polycystin-1 binds Par3/aPKC and controls convergent extension during renal tubular morphogenesis. Nat Commun 4, 2658, doi:10.1038/ncomms3658 (2013).

55 Nishio, S. et al. Loss of oriented cell division does not initiate cyst formation. J Am Soc Nephrol 21, 295-302, doi:10.1681/ASN.2009060603 (2010).

56 Kunimoto, K. et al. Disruption of Core Planar Cell Polarity Signaling Regulates Renal Tubule Morphogenesis but Is Not Cystogenic. Curr Biol 27, 3120-3131 e3124, doi:10.1016/j.cub.2017.09.011 (2017).

57 Skouloudaki, K. et al. Scribble participates in Hippo signaling and is required for normal zebrafish pronephros development. P Natl Acad Sci USA 106, 8579-8584, doi:10.1073/pnas.0811691106 (2009).

58 He, L. L. et al. Yes-Associated Protein (Yap) Is Necessary for Ciliogenesis and Morphogenesis during Pronephros Development in Zebrafish (Danio Rerio). Int J Biol Sci 11, 935-947, doi:10.7150/ijbs.11346 (2015).

59 Hossain, Z. et al. Glomerulocystic kidney disease in mice with a targeted inactivation of Wwtr1. Proc Natl Acad Sci U S A 104, 1631-1636, doi:10.1073/pnas.0605266104 (2007).

60 Makita, R. et al. Multiple renal cysts, urinary concentration defects, and pulmonary emphysematous changes in mice lacking TAZ. Am J Physiol Renal Physiol 294, F542-553, doi:10.1152/ajprenal.00201.2007 (2008).

61 Reginensi, A. et al. Yap- and Cdc42-dependent nephrogenesis and morphogenesis during mouse kidney development. PLoS Genet 9, e1003380, doi:10.1371/journal.pgen.1003380 (2013).

62 Bagherie-Lachidan, M. et al. Stromal Fat4 acts non-autonomously with Dchs1/2 to restrict the nephron progenitor pool. Development 142, 2564-2573, doi:10.1242/dev.122648 (2015).

63 Aguiari, G. et al. Polycystin-1 regulates amphiregulin expression through CREB and AP1 signalling: implications in ADPKD cell proliferation. J Mol Med 90, 1267-1282, doi:10.1007/s00109-012-0902-3 (2012).

64 Yamaguchi, T. et al. Cyclic AMP activates B-Raf and ERK in cyst epithelial cells from autosomal-dominant polycystic kidneys. Kidney Int 63, 1983-1994, doi:10.1046/j.1523-1755.2003.00023.x (2003).

65 Norman, J. Fibrosis and progression of autosomal dominant polycystic kidney disease (ADPKD). Biochim Biophys Acta 1812, 1327-1336, doi:10.1016/j.bbadis.2011.06.012 (2011).

66 Song, C. J., Zimmerman, K. A., Henke, S. J. & Yoder, B. K. Inflammation and Fibrosis in Polycystic Kidney Disease. Results Probl Cell Differ 60, 323-344, doi:10.1007/978-3-319-51436-9_12 (2017).

67 Akhmetshina, A. et al. Activation of canonical Wnt signalling is required for TGF-beta-mediated fibrosis. Nat Commun 3, 735, doi:10.1038/ncomms1734 (2012).

68 Meng, X. M., Tang, P. M., Li, J. & Lan, H. Y. TGF-beta/Smad signaling in renal fibrosis. Front Physiol 6, 82, doi:10.3389/fphys.2015.00082 (2015).

69 Geng, H. et al. Lysophosphatidic acid increases proximal tubule cell secretion of profibrotic cytokines PDGF-B and CTGF through LPA2- and Galphaq-mediated Rho and alphavbeta6 integrin-dependent activation of TGF-beta. Am J Pathol 181, 1236-1249, doi:10.1016/j.ajpath.2012.06.035 (2012).

70 Ono, K., Ohtomo, T., Ninomiya-Tsuji, J. & Tsuchiya, M. A dominant negative TAK1 inhibits cellular fibrotic responses induced by TGF-beta. Biochem Biophys Res Commun 307, 332-337 (2003).

71 Kim, S. I. et al. TGF-beta-activated kinase 1 and TAK1-binding protein 1 cooperate to mediate TGF-beta1-induced MKK3-p38 MAPK activation and stimulation of type I collagen. Am J Physiol Renal Physiol 292, F1471-1478, doi:10.1152/ajprenal.00485.2006 (2007).

72 Jho, E.-h. et al. Wnt/beta-catenin/Tcf signaling induces the transcription of Axin2, a negative regulator of the signaling pathway. Molecular and cellular biology 22, 1172-1183, doi:10.1128/MCB.22.4.1172-1183.2002 (2002).

73 Wielenga, V. J. et al. Expression of CD44 in Apc and Tcf mutant mice implies regulation by the WNT pathway. Am J Pathol 154, 515-523, doi:10.1016/s0002-9440(10)65297-2 (1999).

74 Tetsu, O. & McCormick, F. Beta-catenin regulates expression of cyclin D1 in colon carcinoma cells. Nature 398, 422-426, doi:10.1038/18884 (1999).

75 Shtutman, M. et al. The cyclin D1 gene is a target of the beta-catenin/LEF-1 pathway. Proc Natl Acad Sci U S A 96, 5522-5527 (1999).

76 He, T. C. et al. Identification of c-MYC as a target of the APC pathway. Science 281, 1509-1512 (1998).

77 Rock, R., Heinrich, A. C., Schumacher, N. & Gessler, M. Fjx1: a notch-inducible secreted ligand with specific binding sites in developing mouse embryos and adult brain. Dev Dyn 234, 602-612, doi:10.1002/dvdy.20553 (2005).

78 Tagliabracci, V. S. et al. Secreted Kinase Phosphorylates Extracellular Proteins That Regulate Biomineralization. Science 336, 1150-1153, doi:10.1126/science.1217817 (2012).

79 Sreelatha, A., Kinch, L. N. & Tagliabracci, V. S. The secretory pathway kinases. Biochim Biophys Acta 1854, 1687-1693, doi:10.1016/j.bbapap.2015.03.015 (2015).

Supplementary Figures

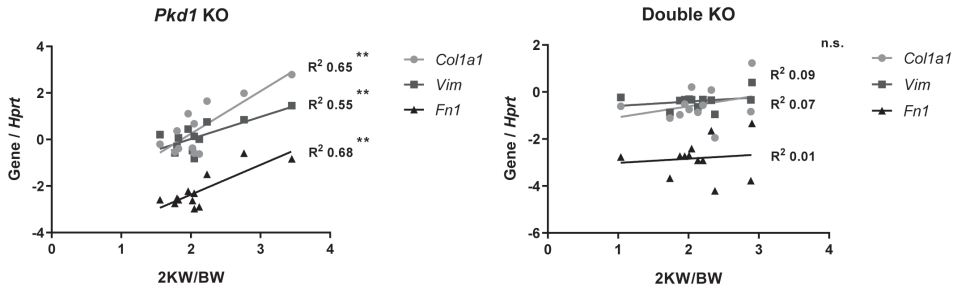

Supplementary Figure 1. Correlation of fibrosis and kidney size in *Pkd1* KO and *Pkd1/Fjx1* double KO mice

Linear regression of 2KW/BW ratio and gene expression normalized on *Hprt* of *Col1a1*, *Vim* and *Fn1* at 10 weeks time point. ** P value <0.01

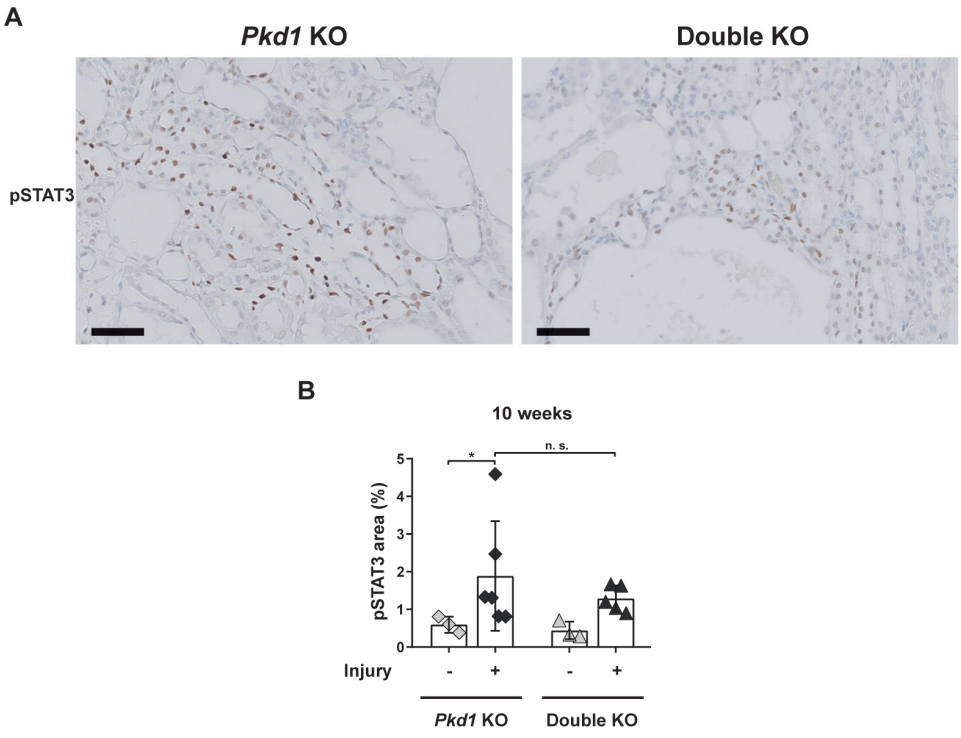

Supplementary Figure 2. Expression of pSTAT3 in *Pkd1* KO and double KO mice

(A) Representative immunostaining for pSTAT3 at 10 weeks after injection of the nephrotoxic compound S-(1,2-dichlorovinyl)-L-cysteine (DCVC) in *Pkd1* KO and *Pkd1/Fjx1* double KO mice kidneys, indicated as ± injury. Scale bars, 50 µm. **(B)** Quantification of pSTAT3 staining. Each symbol shows data from one mouse. Mean ± SD. Two-way ANOVA with Tukey's multiple comparisons test. * P value <0.05.

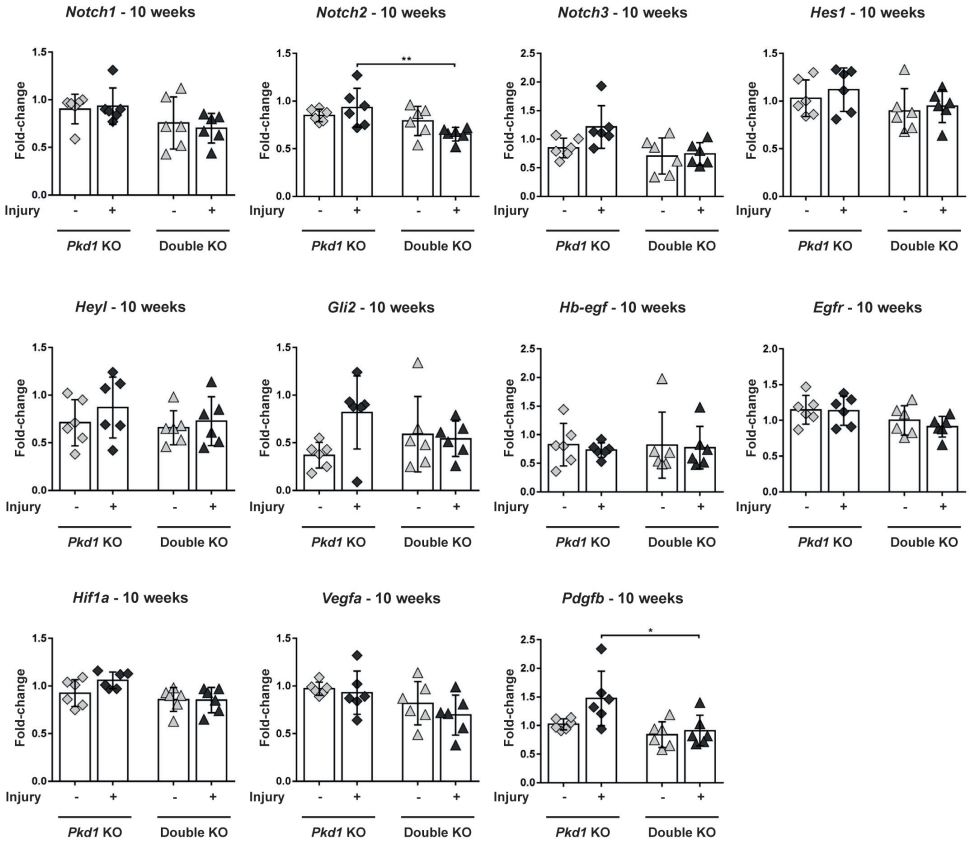

Supplementary Figure 3. Investigation of pathways involved in renal fibrosis at 10 weeks after injection of the nephrotoxic compound S-(1,2-dichlorovinyl)-L-cysteine (DCVC)

Gene expression in *Pkd1* KO mice and *Pkd1*/*Fjx1* double KO mice with or without renal injury induced via injection of DCVC, of Notch target genes (*Notch1*, *Notch2*, *Notch3*); Hedgehog target genes (*Hes1*, *Hey1*, *Gli2*); Egf pathway (*Hb-egf*, *Egfr*); hypoxia pathway (*Hif1a*, *Vegfa*, *Pdgfb*). Each symbol shows data from one mouse. Mean ± SD. Two-way ANOVA with Tukey's multiple comparisons test. * P value <0.05; ** P value <0.01.

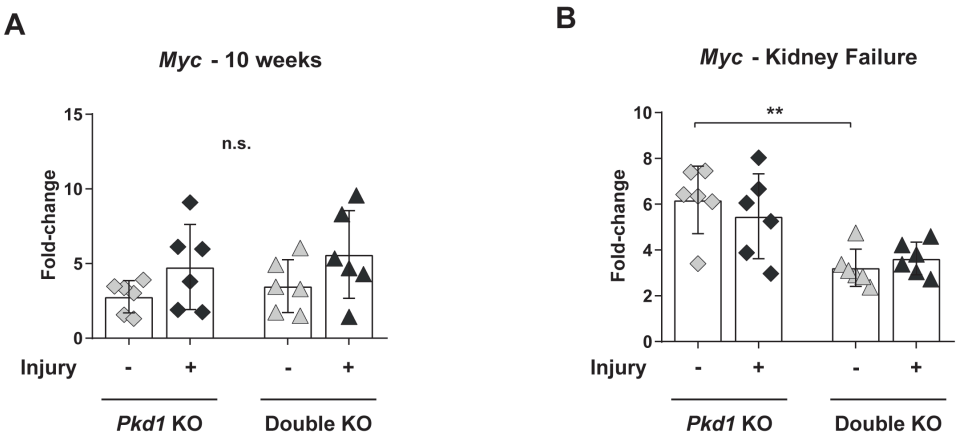

Supplementary Figure 4. Wnt pathway target Myc

(A) Gene expression of *Myc* 10 weeks after injection of the nephrotoxic compound S-(1,2-dichlorovinyl)-L-cysteine (DCVC) or PBS in *Pkd1* KO mice and *Pkd1*/*Fjx1* double KO mice. **(B)** Gene expression of *Myc* at kidney failure in *Pkd1* KO mice and *Pkd1*/*Fjx1* double KO mice. Each symbol shows data from one mouse. Mean ± SD. Two-way ANOVA with Tukey's multiple comparisons test. ** P value <0.01.

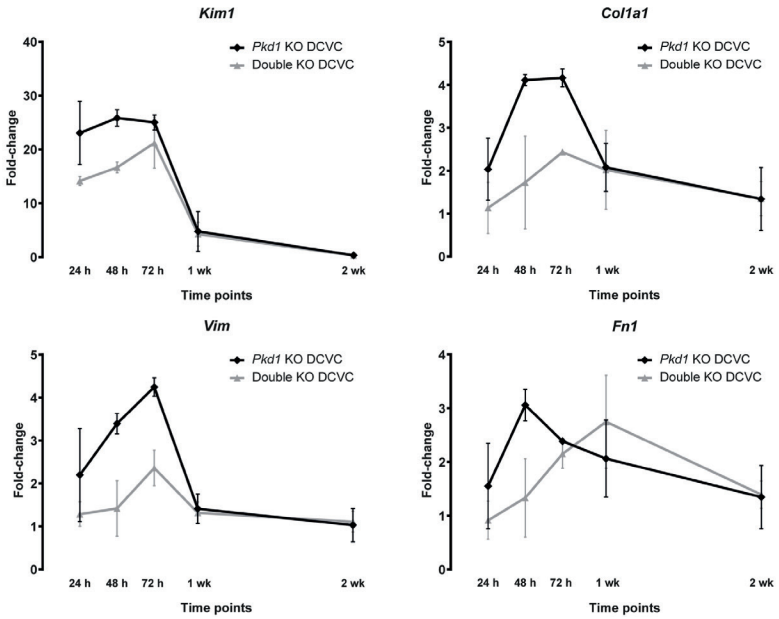

Supplementary Figure 5. Injury and fibrotic genes expression at early time points after injury

Gene expression of *Kim1*, *Col1a1*, *Vim* and *Fn1* at 24 h, 48 h, 72 h, 1 and 2 weeks after S-(1,2-dichlorovinyl)-L-cysteine (DCVC) injection. Each point is the mean of two mice (24 h, 48 h, 72 h) or six mice (1 and 2 weeks) ± SD.

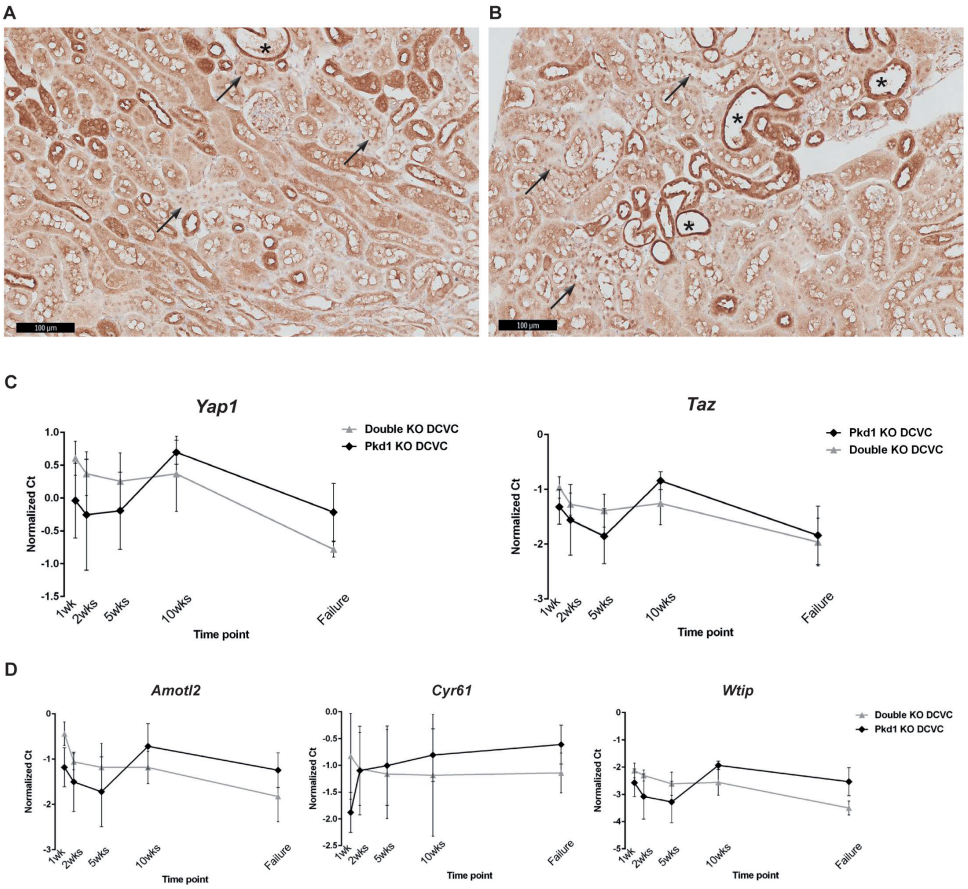

Supplementary Figure 6. Hippo Pathway activation in *Pkd1* KO and *Pkd1*/*Fjx1* double KO mice

(A) Representative immunostaining for Yap1 on kidney tissue in *Pkd1* KO mice after injection of the nephrotoxic compound S-(1,2-dichlorovinyl)-L-cysteine (DCVC) and **(B)** double KO mice after DCVC. In both genotypes, it is possible to observe some dilated tubules which intensely stain for Yap1 and diffuse nuclear localization. Scale bars, 100 µm. Arrows indicate tubules showing nuclear Yap1; asterisks indicate dilated tubules. **(C)** *Yap1* and *Taz* expression during disease progression. **(D)** Gene expression of representative Yap1/Taz targets. Each point is the mean expression of six mice ± SD.

Supplementary Methods

Animal Models

The kidney specific tamoxifen-inducible *Pkd1*-deletion mouse model (*Pkd1*-cKO) has been described previously[1]. The *Fjx1*$^{-/-}$ (*Fjx1* KO) were generated via insertion of the *LacZ* gene followed by a PGK-neo resistance cassette in the single exon of *Fjx1* gene, as described previously[2]. This results in a germline disruption of *Fjx1*. By cross-breeding the kidney specific tamoxifen-inducible *Pkd1*-deletion mice (*Pkd1* KO) with the *Fjx1* KO mice, we generated the *Fjx1*$^{-/-}$/*Pkd1*-cKO double KO mouse model (double KO). Control mice (Wt) carry the *Lox*P site that flanks *Pkd1* exons 2-11 but miss the tamoxifen-inducible Cre recombinase (*Pkd1*^{lox,lox}). Inactivation of the *Pkd1* gene was achieved by oral administration of tamoxifen (5 mg/day, 3 consecutive days) in adult mice that were between 13 to 14 weeks old. Only male mice were used for all the experimental groups. The *Fjx1* KO and the Wt mice also received tamoxifen. Renal injury was induced a week after gene disruption by a single intraperitoneal (i.p.) injection of S-(1,2-dichlorovinyl)-L-cysteine (DCVC) (15 mg/kg) or vehicle. Injury was evaluated by measurement of blood urea level after 40 hours, as described before[3].

Mice were sacrificed at 24, 48 and 72 hours after DCVC injection to study acute injury; at 1, 2, 5 and 10 weeks after DCVC injection to study injury/repair and disease progression and when reaching renal failure indicated by urea levels in the blood equal or over 25 mmol/l. Blood urea nitrogen (BUN) level assessment has been described previously[3]. At sacrifice, mice were weighed; then kidneys were collected and weighed to calculate the 2 kidneys weight to body weight ratios (2KW/BW).

IHC, Golgi position, Cystic and Fibrotic indices

Formalin-fixed paraffin-embedded kidneys were sectioned at 4µm thickness. Section stained with Periodic acid-Schiff (PAS) staining were used to determine cystic index (CI). CI is measured as the ratio of cystic area over the total parenchyma area using Image J software (open source software; National Institutes of Health, Bethesda, MD) and expressed as a percentage. Sections stained with Picro Sirius Red (PSR) staining were used to determine fibrotic index (FI). FI was calculated using a designed color palettes and Photoshop software (Adobe Systems, Inc., San Jose, CA). First a palette was used to remove the pixels of the renal outline area and of the cystic and tubular areas. Then a second palette was used to remove the pixels of the kidney parenchyma except those colored by the PSR staining. Big arteries were manually excluded. The ratio of PSR positive pixels over the total parenchyma pixels was expressed as a percentage and indicated as FI. The same analysis was used to calculate the area positive for alpha Smooth Muscle Actin (αSMA) and for the area positive for F4/80. These antibodies were used for the IHC: rabbit anti αSMA-AP (1:50; Sigma-Aldrich #A5691); rat anti-F4/80 (1:250; Serotec); rabbit anti-Yap (1:800; Cell Signaling Technology #14074), rabbit anti-pStat3 (1:75; Cell Signaling #9145); mouse anti-GM130 (1:500; BD Bioscience

#610822). Anti-rabbit envision HRP (Dako) or anti-rat Immpress HRP (Vector Laboratories) or Alexa 488 goat anti-mouse IgG1 (1:200; Invitrogen) were used as secondary antibodies.
The frequency of cyst size was calculated using Image J software. Pictures of whole kidneys stained with PAS staining were used. The area of the renal outline was removed and then the area of the tubules lumen was measured in pixels and divided in four groups: Normal tubule or mildly dilated tubules up to 1000 pixels; small cysts between 1000 and 2000 pixels; medium cysts between 2000 and 10000 pixels; big cysts more than 10000 pixels.
For the evaluation of the Golgi position as a read-out of the PCP we used a mouse anti-GM130 followed by a secondary Alexa 488 Goat Anti-mouse IgG1 and mounted with Vectashield with Dapi (Vector Laboratories) to visualize the nuclei. From each individual kidney we selected at least 90 tubules with a circularity ≥ 0.995, which was evaluated by Image J software. We scored the Golgi position in relation to the nucleus from 1 to 3, with 1 being the normal peri-centrosomal position at the top of the nucleus towards the lumen, and 3 being very aberrant at the bottom of the nucleus; a score ≥ 2,5 was considered aberrant and the total count was normalized on the number of cells per tubule and expressed as a percentage.

References

1 Lantinga-van Leeuwen, I. S. *et al.* Kidney-specific inactivation of the Pkd1 gene induces rapid cyst formation in developing kidneys and a slow onset of disease in adult mice. *Hum Mol Genet* **16**, 3188-3196, doi:10.1093/hmg/ddm299 (2007).

2 Probst, B., Rock, R., Gessler, M., Vortkamp, A. & Puschel, A. W. The rodent Four-jointed ortholog Fjx1 regulates dendrite extension. *Dev Biol* **312**, 461-470, doi:10.1016/j.ydbio.2007.09.054 (2007).

3 Happé, H. *et al.* Toxic tubular injury in kidneys from Pkd1-deletion mice accelerates cystogenesis accompanied by dysregulated planar cell polarity and canonical Wnt signaling pathways. *Human Molecular Genetics* **18**, 2532-2542, doi:10.1093/hmg/ddp190 (2009).

Supplementary Tables

Supplementary Table 1. List of primer sequences used for qPCR

	Forward	Reverse
Kim1	TCTCTAAGCGTGGTTGCCTT	TGTCTTCAGCTCGGGAATGC
Col1a1	TGACTGGAAGAGCGGAGAGT	AGACGGCTGAGTAGGGAACA
Vim	CCAACCTTTTCTTCCCTGAA	TGAGTGGGTGTCAACCAGAG
Fn1	AATCCAGTCCACAGCCATTCC	CCTGTCTTCTCTTTCGGGTTCA
Acta2	CATCATGCGTCTGGACTTG	ATCTCACGCTCGGCAGTAG
Tgfb	ACTATTGCTTCAGCTCCACAGA	AAGTTGGCATGGTAGCCCTT
Adgre1	GGCAGGGATCTTGGTTATGCT	GCTGCACTCTGTAAGGACACT
Fat4	ACCGATGCAGATGATGGTGTC	ACTCCGTGCTTATCCACTGC
Dchs1	GACAATCGTCCCACCATCCC	AGCCCAACAGTGCATCTTCT
Yap1	TTCCGATCCCTTTCTTAACAGT	GAGGGATGCTGTAGCTGCTC
Taz (Wwtr1)	ATGGACGAGATGGATACAGGTGA	AGACTCCAAAGTCCCGAGGT
Amotl2	ACCAGGAGATGGAGAGCAGATT	GAAGGACCTTGATCACCGCA
Cyr61	CACTGAAGAGGCTTCCTGTCT	CCAAGACGTGGTCTGAACGA
Wtip	TTCATCTGTGACTCCTGTGGGA	TGGCAGTACACTTTCTCACCC
Notch1	GGTGCTCTGATGGACGACAA	TACTGGCTCCTCAAACCGGA
Notch2	AGGCTAACCTGATTGGTTCTGG	AAGCCTCATCCTCAGCCTTG
Notch3	CTGGGAGTCAGTGTCAGAACC	GGTGGACAAATGCAGTAAGCC
Hes1	GGCCTCTGAGCACAGAAAGT	TTGGAATGCCGGGAGCTATC
Heyl	AAGAAGCGCAGAGGGATCATAG	GGGACCAATCGTCGCAATTC
Gli1	CAGCATGGGAACAGAAGGACT	ACCCTGGGACCCTGACATAA
Hb-egf	GAGGAGGACCTGAGCTATAGGAA	AACGTGTAACGAACCACTGTCT
Egfr	GAAGTACAGCTTTGGTGCCACCTG	CTTGCGGATGCCATCTTCTTCCAC
HIF1a	AGTCAGCAACGTGGAAGGTG	GCACGTCATGGGTGGTTTCT
Vegfa	CTCCACCATGCCAAGTGGTC	GTCCACCAGGGTCTCAATCG
Pdgfb	CAAGAGTGTGGGCAGGGTTAT	CCGAATCAGGCATCGAGACA
Axin2	GACAGCGAGTTATCCAGCGA	AGGAGGGACTCCATCTACGC
Jak2	ACCTTTGCTGTTGAGCGAGA	CTTAGTCCCGCTGAGGTTGT
Stat1	TTCCGACACCTGCAACTGAAG	TCTTCGGTGACAATGAGAGGC